

# Therapeutic effect of concentrated growth factor preparation on skin photoaging in a mouse model

Rongrong Zhou<sup>1,2</sup>, Miao Wang<sup>3</sup>,  
Xudong Zhang<sup>2</sup>, Aifen Chen<sup>2</sup>,  
Yanghonghong Fei<sup>2</sup>, Qiming Zhao<sup>4</sup>,  
Danjing Guo<sup>1</sup>, Hui Chen<sup>1</sup> and  
Shusen Zheng<sup>1</sup> 

## Abstract

**Objective:** To establish a nude mouse model of photoaging and study the therapeutic effect of a concentrated growth factor preparation (CGF) on skin photoaging.

**Methods:** CGF was prepared from blood from Sprague–Dawley rats. A skin photoaging nude mouse model was developed using UV irradiation combined with the photosensitizer, 8-methoxypsoralen. Mice were divided randomly into seven groups ( $n = 6$  per group): normal control, photoaging, mock treatment, saline treatment, CGF treatment, Filoca 135HA treatment, and plasma skin regeneration system irradiation (the latter two were positive controls). Body weight and skin appearance were observed and pathological changes were determined by hematoxylin and eosin staining. Fiber elasticity was evaluated by Weigert staining. Expression levels of proliferating cell nuclear antigen (PCNA) and matrix metalloproteinase I (MMP1) were determined by immunohistochemistry.

**Results:** A mouse model with typical features of photoaging skin was successfully developed. CGF significantly improved the skin appearance, wrinkle scores, pathological changes, and fiber elasticity, and increased PCNA and decreased MMP1 expression levels in photoaging mice, comparable to the two positive controls.

<sup>1</sup>Division of Hepatobiliary and Pancreatic Surgery, Department of Surgery, First Affiliated Hospital, School of Medicine, Zhejiang University, Hangzhou, China

<sup>2</sup>Joint Service Support Force 903 Hospital, Hangzhou, China

<sup>3</sup>ArtBeauty Cosmetology Clinic, Guangzhou, China

<sup>4</sup>Zhejiang Hospital, Hangzhou, China

## Corresponding author:

Shusen Zheng, Division of Hepatobiliary and Pancreatic Surgery, Department of Surgery, First Affiliated Hospital, School of Medicine, Zhejiang University, No. 79 Qingchun Road, Hangzhou 310003, China.

Email: shusenzheng@zju.edu.cn



**Conclusion:** CGF can improve the symptoms of skin photoaging in mice, suggesting that it may have applications in the treatment of skin aging in humans.

### Keywords

Concentrated growth factor, skin photoaging, photoaging mouse model, pathological change, elastic fiber, elasticity

Date received: 29 April 2020; accepted: 9 September 2020

## Introduction

Skin aging is a complex biological phenomenon mediated by both intrinsic and extrinsic processes. Intrinsic factors include genetics and age, whereas extrinsic environmental factors include photodamage, smoking, air pollution, occupation, and lifestyle.<sup>1-5</sup> UV-induced skin aging, referred to as photoaging, accounts for approximately 80% of facial aging.<sup>1,3</sup>

Oxidative stress is the primary cause of extrinsic aging or photoaging.<sup>3</sup> Several factors, including nuclear factor- $\kappa$ B, epidermal growth factor (EGF), mitogen-activated protein kinase, matrix metalloproteinase (MMP), and interleukin-1 $\beta$ , are implicated in the etiopathogenesis of skin photoaging.<sup>4,6</sup> However, MMPs are the final effectors of collagen degradation and pro-collagen inhibition, leading to loss of collagen and consequent skin aging.<sup>6</sup> Skin photoaging is involved in the occurrence and progression of various dermatological conditions, including solar keratosis, chronic optical cheilitis, photoelastic fibrosis, melanoma, basal cell carcinoma, solar freckle-like mites, and squamous cell carcinoma.<sup>7</sup> Strategies that can effectively delay and prevent skin photoaging are thus of important clinical significance.

The clinical features of photoaging include skin atrophy, coarse wrinkles, leathery skin, lentigines, yellowish-brown

appearance, telangiectasia, hyperpigmentation, and photodermatitis, while the histological features include elastosis, collagen fragmentation, irregular epidermal thickness, increased local concentrations of glycosaminoglycans and proteoglycans, increased expression of inflammatory markers (e.g., mast cells, eosinophils, mononuclear cells), and melanogenesis.<sup>6,8</sup> Among these, elastosis is a characteristic feature of skin photoaging. There are two major approaches to managing photoaging: prevention of UV damage via photoprotection and sunscreens, and medications to reverse skin damage (e.g., topical retinoids, 5-fluorouracil cream, and cosmeceuticals containing antioxidants or  $\alpha$ -hydroxy acids).<sup>6,9</sup> Clinical treatments for moderate to severe photoaging include intense pulse light,<sup>10-12</sup> dermabrasion,<sup>13,14</sup> chemical peeling,<sup>15,16</sup> botulinum toxin injections,<sup>17</sup> and laser resurfacing.<sup>18</sup>

Botulinum toxin injections are an effective therapeutic approach to skin photoaging with widespread clinical applications,<sup>17</sup> while hyaluronic acid and autologous blood concentrate are also used to treat photoaging. Platelet-rich plasma (PRP) and platelet-rich fibrin (PRF) are first- and second-generation derivatives of blood concentrates, respectively,<sup>19</sup> both of which contain many growth factors, including platelet-derived growth factor (PDGF), insulin-like growth factor (IGF-1),

transforming growth factor- $\beta$ 1 (TGF $\beta$ 1), basic fibroblast growth factor (bFGF), vascular endothelial growth factor (VEGF), and EGF,<sup>20</sup> which can promote tissue repair and regeneration.<sup>19</sup> PRP and PRF have diverse applications in different medical fields such as hematology, maxillofacial surgery, and musculoskeletal restoration in sports medicine.<sup>19</sup> These platelet concentrates have recently been used in dermatology, mainly for tissue regeneration, wound healing, scar revision, skin rejuvenation, and alopecia.<sup>21,22</sup> The growth factors in PRP can stimulate fibroblast activation and induce the synthesis of collagen and other components of the extracellular matrix and can thus alleviate wrinkling and elastosis in skin photoaging.<sup>23</sup>

Concentrated growth factor (CGF) is the latest blood concentrate product. CGF contains levels of bFGF comparable to and higher than those in PRF and activated PRP, respectively,<sup>24</sup> while levels of the other growth factors are comparable among all three concentrates.<sup>24</sup> Current research into CGF has focused on tissue regeneration. CGF can increase the proliferation and promote osteogenic differentiation and the angiogenic potential of periosteum-derived cells.<sup>25</sup> It can also promote the proliferation, migration, and differentiation of human dental stem pulp cells exposed to lipopolysaccharide,<sup>26</sup> and induce regeneration of the dentine-pulp complex of immature teeth *in vivo*. In addition, CGF can upregulate the *in vivo* proliferation and secretion of neurotrophic factors from Schwann cells and promote functional recovery following peripheral nerve injuries.<sup>27</sup> These findings suggest the potential application of CGF in bone grafting and regenerative endodontics. Moreover, CGF is superior to PRF and PRP in promoting bone healing.<sup>28</sup> A recent meta-analysis showed that CGF, but not PRP, influenced therapeutic outcomes in the management of gingival

recession.<sup>29</sup> However, research into the effect of CGF on photoaging is lacking. The current study was conducted to investigate the therapeutic effect of CGF on photoaging in a nude mouse model.

## Methods

### Animals

Specific pathogen-free, male Sprague-Dawley rats ( $n = 10$ ; weight: 278.5–290.3 g) and male BALB/c nude mice ( $n = 42$ ; weight: 17.5–21.8 g), both 8 weeks old, were purchased from the Zhejiang Academy of Medical Sciences (Zhejiang, China). Food and water were provided *ad libitum* and the experimental animals were housed at 20°C to 25°C under a 12-hour light/dark cycle and allowed to adapt to their environment for 1 week before the experiments. The study protocol was approved by the animal ethics committee of the First Affiliated Hospital, College of Medicine, Zhejiang University (No. 2017-565-1).

### Preparation of CGF

Rats were administered general anesthesia (7% chloral hydrate 0.4 mL/100 g) and 11 mL of blood was collected from the inferior vena cava, of which 2 mL was preserved as a control and 9 mL was processed as follows: centrifugation at  $300 \times g$  for 2 minutes,  $240 \times g$  for 4 minutes,  $300 \times g$  for 4 minutes, and  $380 \times g$  for 3 minutes. Centrifugation produced three separate layers: an upper light-yellow layer of serum, a middle yellow layer of CGF, and a sedimented pellet of red blood cells and debris. The CGF and the thin, growth factor-rich film between the upper and middle layers were collected for further experiments. All rats were sacrificed by cervical dislocation after blood sample collection.

### **Enzyme-linked immunosorbent assay (ELISA)**

The concentrations of EGF, VEGF, TGF $\beta$ 1, bFGF, IGF-1, and PDGF in CGF were determined using commercially available ELISA kits (Mlbio, Shanghai, China) according to the manufacturer's instructions.

### **Animal model of photoaging and treatment**

A mouse model of photoaging was developed using UVA irradiation together with 0.1% 8-methoxypsoralen (8-MOP) as a photosensitizer. Briefly, the dorsal skin of the nude mouse was covered with 0.1% 8-MOP (Huapont Pharm, Chongqing, China) and irradiated with a UVA lamp (350–460 nm, 40 W;  $13 \times 102 \mu\text{W}/\text{cm}^2$ ) placed 15 cm from the animal. The mice underwent irradiation once daily, 5 days a week, for 2 weeks. In the first week, mice were irradiated for 1, 2, 3, 4, and 5 hours on days 1 to 5, and the irradiation was then stopped for 2 days. The mice were irradiated again from days 8 to 12, for 5 hours every day. The total UVA irradiation intensity was  $172\text{J}/\text{cm}^2$ . During irradiation, skin changes such as erythema, scaling, erosion, blisters, and pigmentation, as well as skin elasticity and texture, were monitored closely. In the event of blistering, rupture, and erosion of the skin during the experiment, irradiation was stopped and the dorsal skin was disinfected with iodophor twice a day. Irradiation was resumed when the symptoms disappeared.

Nude mice were divided randomly into seven groups ( $n = 6$  per group): normal control, UVA+8-MOP (photoaging), UVA+8-MOP+ null injection (mock), UVA+8-MOP+saline injection (saline; total of 0.6 mL saline injection [ $0.2\text{ mL} \times 3$ ]), UVA+8-MOP+CGF injection (CGF; total of 0.6 mL CGF [ $0.2\text{ mL} \times 3$ ] injection),

UVA+8-MOP+Filoca 135HA injection (Filoca 135HA [Filorgan, France]; total of 0.6 mL Filoca 135HA [ $0.2\text{ mL} \times 3$ ] injection, positive control), and UVA+8-MOP+plasma skin regeneration system irradiation (PSR; irradiated for 2 minutes at each square with total dose of 3.0 J, positive control). The largest volume of liquid tolerated in  $1\text{ cm}^2$  skin in our preliminary experiments was 0.2 mL, and we therefore used a maximum volume of 0.2 mL in all injection groups in the present study.

In each group, the dorsal skin of each mouse was marked symmetrically into four squares (each measuring  $1 \times 1\text{ cm}^2$ ) along the dorsal spine. One randomly selected square was used to evaluate the photoaging model and the other three squares were subjected to injection or irradiation, according to the different groups. After 1 month, all the mice were sacrificed by cervical dislocation and one square was randomly selected for histochemical examination (hematoxylin and eosin [HE] and Weigert staining).

### **General and gross examinations**

The general condition, including diet, sleep, bowel movements, mental status, and weight changes, was observed for each mouse. Changes in the gross appearance of the dorsal skin were also observed, including skin texture, pigmentation, wrinkles, elasticity, and ulceration. Wrinkles were scored as previously reported:<sup>30</sup> 0 points, no thick wrinkles; 2 points, few superficial and thick wrinkles across the back; 4 points, many superficial and thick wrinkles across the back; and 6 points, deep long wrinkles across the back. We used a magnifying glass skin detector (magnification,  $80\times$  and  $200\times$ ; HOT, Shenzhen, China) to detect changes in the dorsal skin, including skin texture, pigmentation, wrinkles, elasticity, and ulceration.

## Histochemistry

Skin samples were fixed in 4% formaldehyde for 24 hours, then dehydrated, cleared, infiltrated, embedded in paraffin, and cut into 4- $\mu$ m-thick serial sections. The sections were dewaxed and subjected to HE or Weigert staining. Slides with HE-stained skin sections were observed under an Olympus BX51 light microscope (100 $\times$ ; Olympus, Japan), and the histological structure and changes in the epidermis and dermis, as well as the arrangement of collagen fibers in the dermis, were documented. Five fields were randomly selected from each slide and the thickness of the dermis was measured using Image Pro 6.0 software. The Weigert-stained slides were observed under an Olympus BX51 light microscope (400 $\times$ ) to determine the appearance of the elastic fibers. Denaturation of the elastic fibers was classified according to Kligman's grading system:<sup>31</sup> 0, no change; 1+, increase without thickening; 2+, some hyperplasia with thickening and distortion; 3+, obvious hyperplasia, thickening, distortion, and often bifurcation; and 4+, dermis completely replaced by high-density, thickened, twisted, disordered fibers with irregular amorphous deposits.

## Immunohistochemistry

The dewaxed slides were subjected to heat-mediated antigen retrieval with citric acid buffer (pH 6.0) followed by blocking with 5% to 10% goat serum. The slides were incubated overnight at 4°C with primary antibodies to proliferating cell nuclear antigen (PCNA; ab29, 1:10,000; Abcam, Cambridge, MA, USA) or MMP1 (ab137332, 1:250; Abcam), followed by horseradish peroxidase-labeled secondary antibodies (SAB43714; 1:20,000; Bioswamp, Wuhan, China) for 20 minutes at 37°C. The slides were finally stained with diaminobenzidine and observed

under a light microscope. The number of positive cells per 100 cells (excluding proliferating cells of the sebaceous gland and hair follicles) was counted. The proliferation index (PI) was calculated as follows:  $PI = \text{PCNA-positive cell number} / \text{total cell number}$ . For MMP1, the positive cell percentage (0, 0%; 1, <25%; 2, 25% to 50%; 3, 51% to 75%; and 4, >75%) and staining intensity (0, no color; 1, light yellow; 2, brown; and 3, tan) were scored and four grades were defined according to the sum of the positive cell percentage and staining intensity: 0–3, negative or weakly positive, and  $\geq 4$ , positive and strongly positive.

## Statistical analysis

All data were expressed as mean  $\pm$  standard deviation and analyzed using SPSS Statistics for Windows, version 20.0 (SPSS Inc., Chicago, IL, USA). Between-group comparisons were analyzed using independent *t*-tests or one-way ANOVA tests. Pre- and post-treatment skin appearances were compared by paired *t*-tests or  $\chi^2$  tests. A *P*-value < 0.05 was considered significant.

## Results

### Cytokines in CGF

Levels of EGF, VEGF, TGF $\beta$ 1, bFGF, IGF-1, and PDGF were significantly higher in CGF than in the control whole-blood sample (Table 1), indicating successful preparation of CGF for use in subsequent experiments.

### Establishment of photoaging mouse model

All mice had normal diet, sleep, and bowel movements and appeared healthy. Mice in the photoaging model group had significantly more weight loss than the normal

**Table 1.** Concentrations of growth factors in concentrated growth factor preparation.

Growth factor	Blood	CGF	P value
EGF (pg/mL)	465.20 ± 93.49	1035.97 ± 343.50	0.003
bFGF (pg/mL)	20.04 ± 3.06	34.83 ± 10.39	0.003
VEGF (pg/mL)	145.39 ± 32.05	271.32 ± 147.03	0.043
PDGF (pg/mL)	21.37 ± 4.42	42.74 ± 18.97	0.020
IGF-I (ng/mL)	30.68 ± 6.00	64.28 ± 31.79	0.029
TGFβ1 (pg/mL)	205.87 ± 27.98	407.43 ± 210.01	0.029

CGF, concentrated growth factor; EGF, epidermal growth factor; bFGF, basic fibroblast growth factor; VEGF, vascular endothelial growth factor; PDGF, platelet-derived growth factor; IGF-I, insulin-like growth factor-I; TGFβ1, transforming growth factor-β1.

control group (body weight: 20.78 ± 1.43 g vs 23.58 ± 1.80 g,  $P < 0.01$ ; Figure 1a).

Mice in the normal control group had smooth, delicate, lustrous skin with good elasticity, and no pigmentation, obvious wrinkles, or ulceration (Figure 1b). The magnifying glass skin detector revealed clear and regular rhombic skin texture with little desquamation in the normal control group (Figure 1b). In contrast, mice in the photoaging model group had dry, rough, thickened, pigmented skin, with poor elasticity and evident wrinkles with deep furrows and desquamation (Figure 1b). The skin appeared porcelain white with dry desquamation resembling fish scales under magnification (Figure 1b). Wrinkling was significantly higher in the model compared with the normal control group (4.33 ± 1.31 vs 0.33 ± 0.82,  $P < 0.01$ ; Figure 1c).

HE staining showed an intact epidermis with neatly arranged epidermal cells and well-demarcated epidermal processes and dermal papilla, and a dermis with evenly and densely distributed wavy fibers in the normal control group. However, mice in the photoaging group had atrophic epidermis with wavy or even parallel cells, and a dermis with extensively disrupted and denatured fibers, accompanied by inflammatory cell infiltration (Figure 1d). The thickness of the dermis was significantly reduced in the model compared with the control group

(283.42 ± 27.67 μm vs 405.87 ± 93.32 μm,  $P < 0.01$ ; Figure 1e).

Weigert staining showed that the dermis in the normal control group had finer upper elastic fibers and thicker middle and lower elastic fibers, running roughly parallel to the epidermis, while mice in the photoaging groups presented with typical skin photoaging of solar elastic fiber denaturation, including thicker and larger elastic fibers in the reticular and dermal papilla layers, with some entangled, bifurcated, and broken hyperplastic elastic fibers, and increased formation of elastic fibers around the skin appendages (Figure 1f). The skin elastic fiber denaturation score was significantly higher in the model groups compared with the normal control group (3.33 ± 0.67 vs 0.83 ± 0.75,  $P < 0.01$ ; Figure 1g).

The PI value was significantly lower in the model group than in the normal control group (23.86 ± 5.19 vs 43.33 ± 8.14,  $P < 0.01$ ; Figure 1h, i), and the MMP1-positivity rate was also significantly lower (16.7% vs 86.7%,  $P < 0.01$ ; Figure 1j). These results suggest the successful construction of a skin photoaging mouse model.

### CGF treatment improved skin appearance

Mice in the normal control group had smooth, delicate, lustrous skin with no

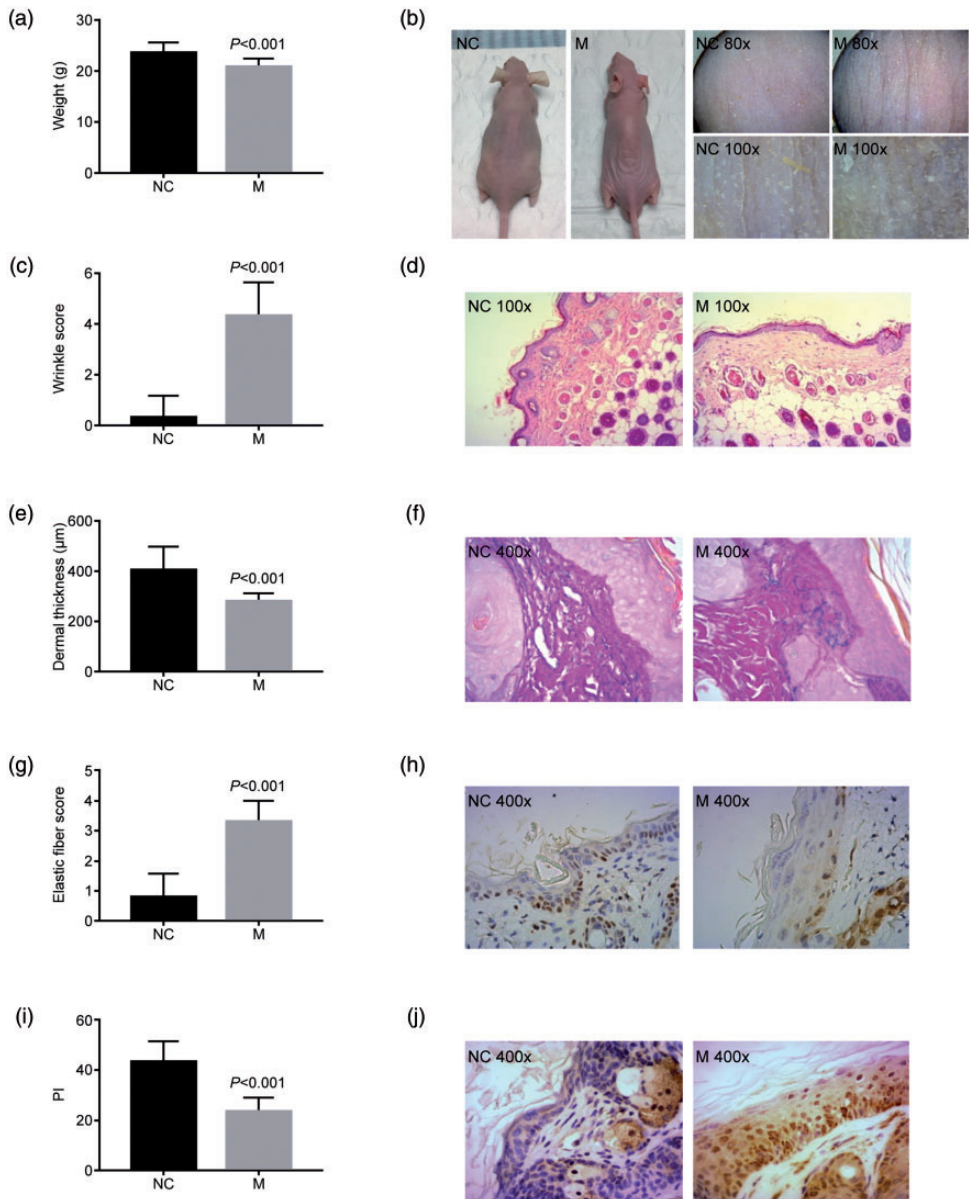


**Figure 1.** Features of a novel mouse model of photoaging. A mouse model of skin photoaging was developed using UV irradiation combined with the photosensitizer, 8-methoxypsoralen. (a) Mouse body weight, (b) gross skin appearance, (c) wrinkle score, (d) hematoxylin and eosin staining, (e) dermal thickness, (f) Weigert staining, (g) elastic fiber score, (h) proliferating cell nuclear antigen, (i) proliferation index, and (j) matrix metalloproteinase I expression were evaluated in control and photoaging mice.  $P$  value compared with the NC group.

NC, normal control; M, photoaging model group; PI, proliferation index.

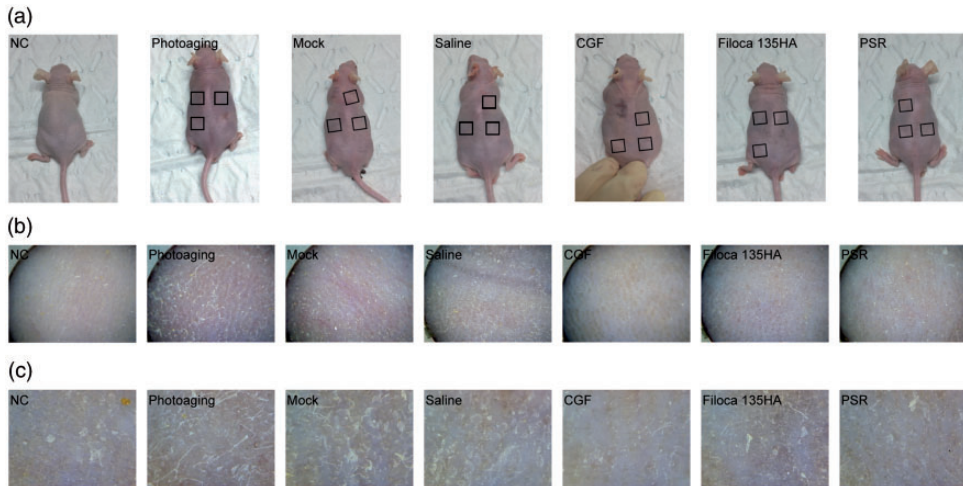


**Figure 2.** Effects of treatments on gross appearance of skin in a mouse model of photoaging. Concentrated growth factor treatment improved skin appearance. (a) Overview; (b)  $\times 80$ ; (c)  $\times 200$ . NC, normal control; CGF, concentrated growth factor; PSR, plasma skin regeneration system irradiation.

pigmentation, obvious wrinkles, or ulceration, and with good elasticity (Figure 2). The appearance of the skin in the mock and saline-treated groups was similar to that of mice in the untreated photoaging group: the skin was dry and rough, with poor elasticity, obvious pigmentation and desquamation, with no obvious texture. The skin was also thinner than before UV irradiation. CGF treatment improved the skin appearance, resulting in a slightly thicker and softer texture, similar to that in the mice treated with Filoca 135HA and PSR. When observed under a magnifying glass, the skin texture in the normal control group was clear with little desquamation, whereas the skin in the photoaging mice was porcelain white with dry desquamation resembling fish scales. The skin appearance in the mock and saline-treated groups was slightly better than in the photoaging group. However, CGF treatment resulted in smoother skin with less-apparent scaling, although fine grain-like protrusions, skin textural changes, and uneven pigmentation were observed.

Filoca 135HA and PSR treatments showed similar effects. Overall, these three treatments all improved the skin appearance but did not restore it to normal.

#### *CGF treatment improved pathological skin changes*

Photoaging model mice had variously thickened epidermis, incomplete skin structure, fuzzy layering, flat junctions between the epidermis and dermis, reduced dermal thickness, denatured and homogenized collagen fibers with reduced content, increased proliferating fibroblasts, and homogenized matrix inflammatory cell infiltration (Figure 3a). Mice in the mock and saline-treated groups showed slight improvements in skin structure. CGF treatment resulted in an intact skin structure with a clear cell layer and significantly thickened dermis, with increased deposits of new collagen, similar to the appearance after Filoca 135HA and PSR treatments.

CGF, Filoca 135HA, and PSR all significantly improved the thickness of the dermis compared with the photoaging group (all



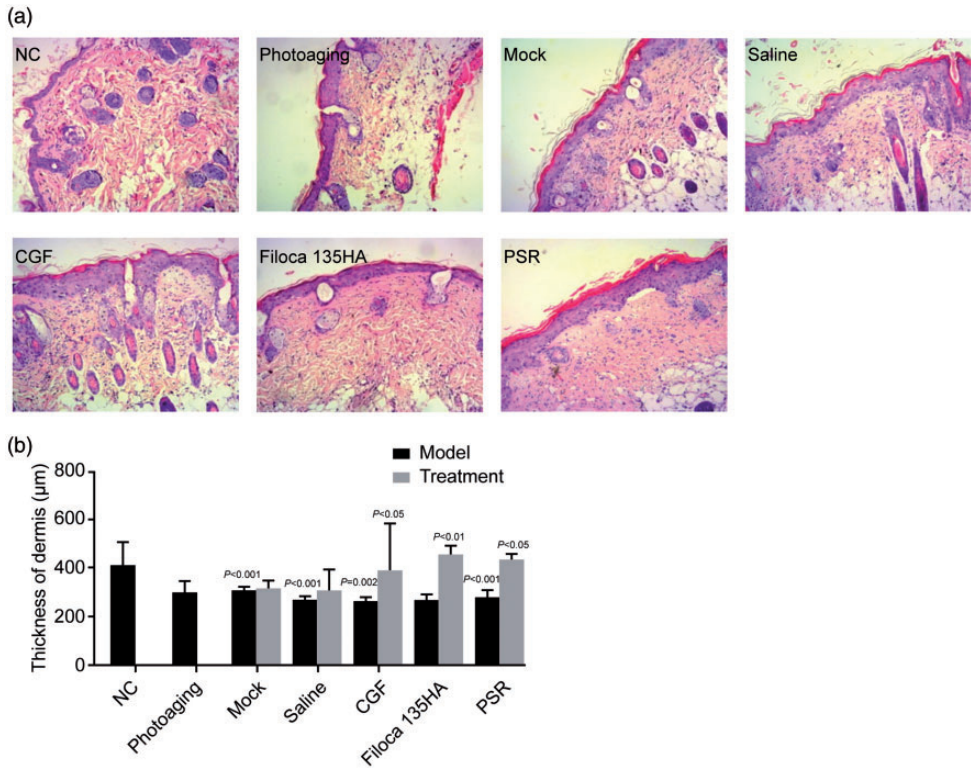


**Figure 3.** Effects of treatments on skin pathology and dermal thickness in a mouse model of photoaging. Concentrated growth factor treatment improved skin pathological changes, indicated by (a) hematoxylin and eosin staining ( $\times 400$ ) and (b) dermal thickness.  $P$  values above black columns compared with the NC group;  $P$  values above grey columns compared with respective model group. NC, normal control; CGF, concentrated growth factor; PSR, plasma skin regeneration system irradiation.

$P < 0.01$ ), comparable to the normal control group (Figure 3b). These results indicated that the dermis in photoaging mice was normalized by these treatments.

### CGF treatment improved elastic fiber structure

Photoaging model mice showed increased and thickened elastic fibers in the reticular layer and dermal papillary layer, some of which were bifurcated, entangled, and broken. There was also increased deposition of elastic fibers around the skin appendages. Mice in the mock and saline-treated groups

showed similar changes. However, the number and density of the dermal elastic fibers increased after CGF, Filoca 135HA, and PSR treatments (Figure 4a).

These three treatments significantly lowered the denaturation score (all  $P < 0.05$ ) compared with the photoaging groups (Figure 4b), indicating that the treatments improved the elasticity of photoaged skin.

### CGF treatment promoted skin cell proliferation

PCNA is a marker of cell proliferation.<sup>32</sup> We therefore calculated the PI value to

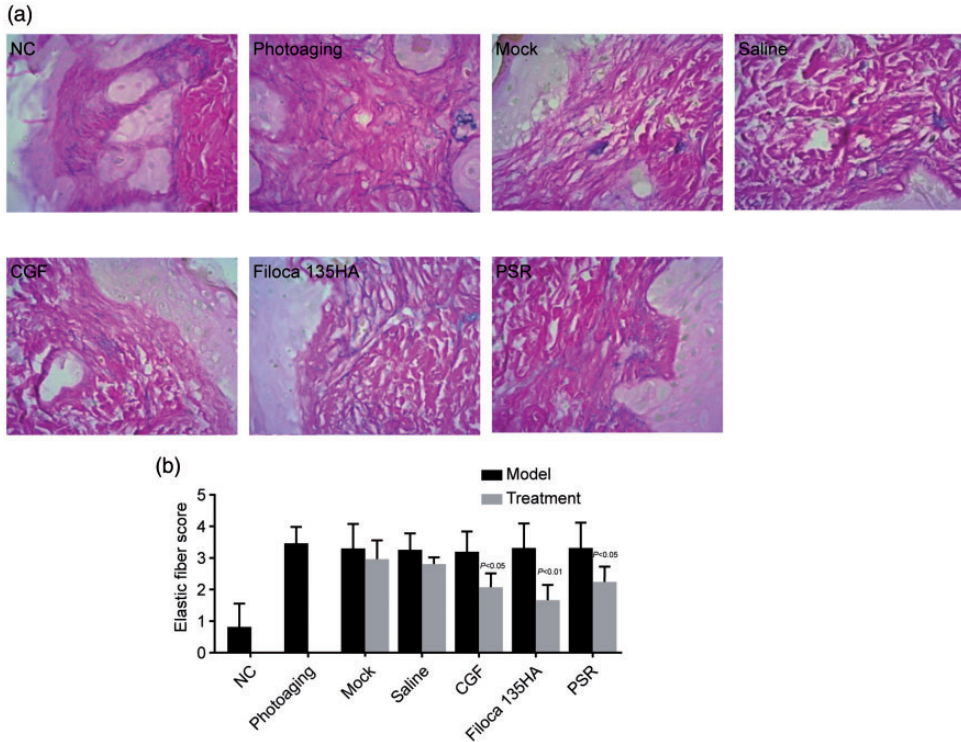


**Figure 4.** Effects of treatments on fiber elasticity in a mouse model of photoaging. Concentrated growth factor treatment improved fiber elasticity. (a) Weigert staining ( $\times 400$ ); (b) elastic fiber score.  $P$  value compared with respective model group.

NC, normal control; CGF, concentrated growth factor; PSR, plasma skin regeneration system irradiation.

investigate the proliferation of skin cells. PI values in the photoaging skin groups increased slightly following mock and saline treatments ( $P < 0.05$ ), while CGF treatment significantly improved the PI value, similar to the values following Filoca 135HA and PSR treatments (all  $P < 0.05$ ; Figure 5), indicating these three treatments promoted the proliferation of skin cells in photoaging model mice.

#### CGF treatment increased MMP1 expression

Levels of MMP1 were significantly increased in photoaging model mice compared with normal controls, and CGF

treatment significantly decreased MMP1 expression levels, similar to those following Filoca 135HA and PSR treatments (all  $P < 0.05$ ; Figure 6), indicating that these treatments effectively alleviated skin aging in photoaging model mice.

## Discussion

In the present study, we successfully developed a mouse model of photoaging and explored the therapeutic effect of CGF on photoaging using this model. Our results showed that CGF significantly improved skin appearance, pathological changes, and the elastic fiber structure of the skin, thereby promoting the proliferation of

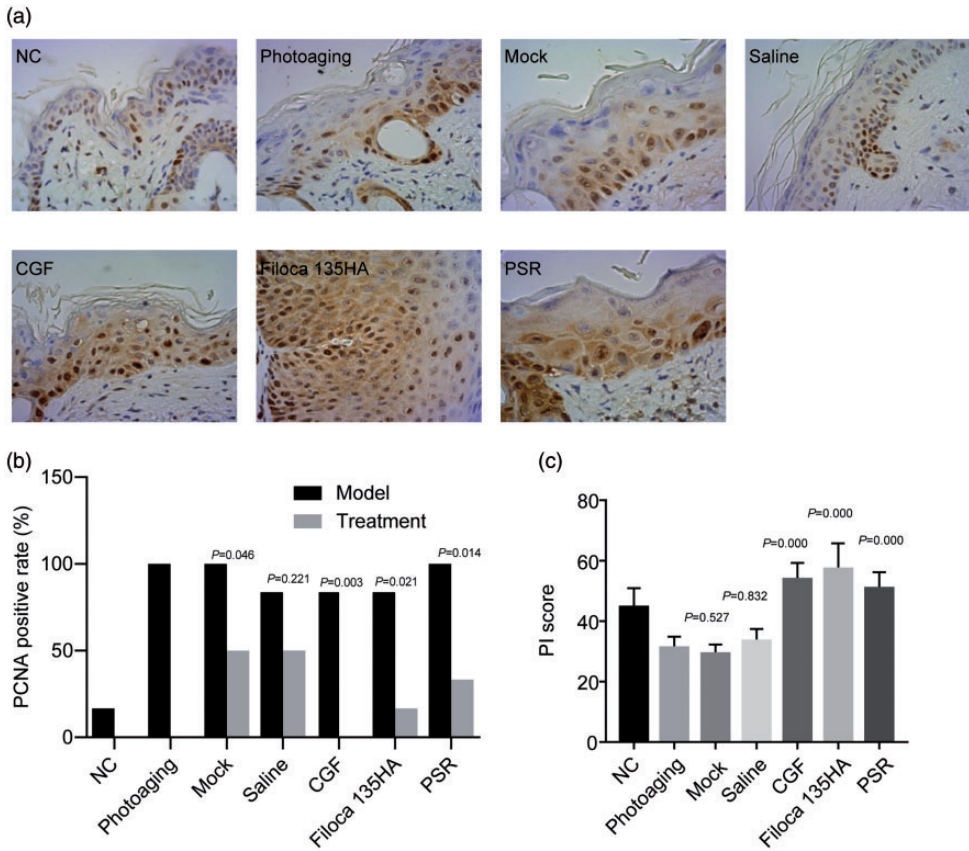


**Figure 5.** Effects of treatments on expression levels of proliferating cell nuclear antigen (PCNA) in a mouse model of photoaging. Concentrated growth factor treatment increased the expression levels of PCNA. (a) Immunohistochemistry ( $\times 400$ ); (b) PCNA-positivity rate; (c) proliferation index score. *P* value in b compared with respective model group; *P* value in c compared with photoaging group. NC, normal control; CGF, concentrated growth factor; PSR, plasma skin regeneration system irradiation; PI, proliferation index.

skin cells and thus effectively inhibiting skin aging in this mouse model.

The hairless mouse model is currently the most widely used skin photoaging model. Its advantage is that there is no body hair to interfere with the UV light, making it easier to simulate chronic light damage. However, the hairless mouse is a mutant mouse without natural hair protection. These mice seldom venture out in daylight and therefore have almost no photodamage, in stark contrast to the

long-term exposure of humans to UV light, which leads to gradual skin photoaging. Hairless mice are thus not an ideal animal model for photoaging studies.<sup>33</sup> A recent study established a photoaging animal model using nude mice,<sup>34</sup> and we therefore used BALB/c nude mice to establish the photoaging model in the current study.

The dose, interval, total irradiation period, and cumulative dose of UV radiation used in previous studies differed. Kim

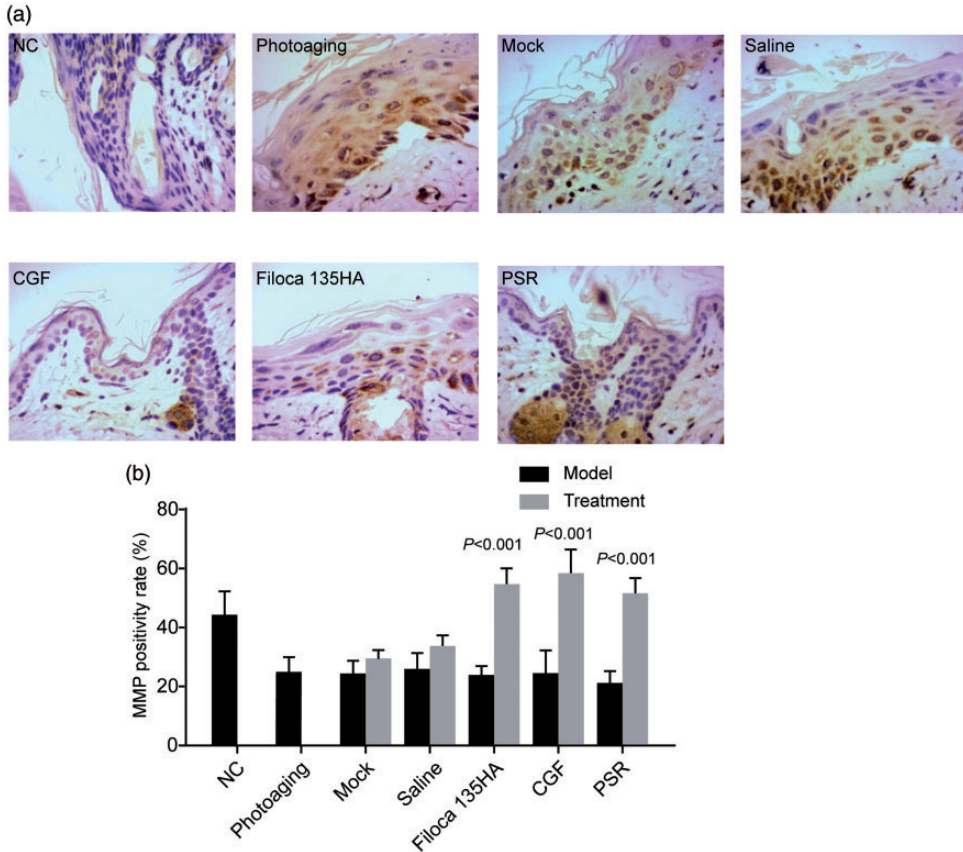


**Figure 6.** Effects of treatments on expression levels of matrix metalloproteinase I (MMP1) in a mouse model of photoaging. Concentrated growth factor treatment decreased the expression levels of MMP1. (a) Hematoxylin and eosin staining ( $\times 400$ ); (b) MMP1-positivity rate. *P* values compared with NC group. NC, normal control; CGF, concentrated growth factor; PSR, plasma skin regeneration system irradiation.

et al.<sup>35</sup> irradiated the skin on the back of female albino nude mice with  $100 \text{ J/cm}^2$  UVA three times a week for 10 weeks, up to a cumulative dose of  $3 \text{ kJ/cm}^2$ , resulting in rough, slack, wrinkled skin. Ropke et al.<sup>36</sup> irradiated albino nude mice with  $70 \text{ mJ/cm}^2$  UVB five times a week for 22 weeks, with a cumulative dose of  $6.16 \text{ J/cm}^2$ , and noted increased, deepened wrinkles, and thickened epidermis, loosened stratum corneum, and a thicker granular layer on HE staining. Aitken et al.<sup>37</sup> irradiated the skin on the back of female nude mice with 97.1% UVA and 2.9% UVB

five times a week for 20 weeks, with a cumulative dose of  $1630 \text{ J/cm}^2$ . After irradiation, the skin appeared rough and wrinkled, and HE staining showed a thickened epidermis, while immunohistochemistry showed an increase in extracellular matrix and a decrease in fibroblasts and collagen. Sumiyoshi et al.<sup>38</sup> irradiated the back of male hairless mice with UVB three times a week with an initial dose of  $36 \text{ mJ/cm}^2$ , increasing to  $54 \text{ mJ/cm}^2$  in the first 4 weeks, and gradually increasing to  $180 \text{ mJ/cm}^2$  over 16 to 19 weeks, with a cumulative dose of  $80 \text{ mJ/cm}^2$ ; however,

no acute photodamage was observed. The above studies suggest that photoaging modeling using a gradually increasing radiation dose can avoid acute photodamage, which might affect the accuracy of the results. We therefore exposed the nude mice to a gradually increasing radiation dose in the present study. The previous reports used varying radiation doses over long time periods (mean 10–22 weeks). We therefore applied a photosensitizer (8-MOP) that was easily activated by UVA to accelerate skin photoaging. Finally, we used a small-dose-escalation method and extended the irradiation time to 2 weeks to avoid acute skin photodamage.

Certain criteria are used to validate skin photoaging animal models. Morphological changes in skin photoaging and changes in the expression levels of molecular biomarkers have previously been used as the main evaluation criteria. It is generally believed that degeneration of dermal elastic tissue is the most prominent histological feature of skin photoaging models, and MMP is one of the best-recognized markers associated with skin photoaging.<sup>5,6</sup> In the present study, we therefore evaluated the appearance and texture of the skin using the naked eye and under a magnifying glass, and used HE and Weigert staining, as well as immunohistochemical analysis of PCNA and MMP1, to verify the successful development of the skin photoaging nude mouse model. The results showed that the skin in the model mice was dry, rough, and thickened with poor elasticity, pigmentation, obvious wrinkles, deepened grooves, and desquamation, with a much higher wrinkle score compared with normal control mice. HE staining showed extensive destruction and denaturation of collagen fibers with partial homogenization, decreased dermal thickness, and increased and thickened elastic fibers that were broken, entangled, and bifurcated, characteristic of solar elastic fiber degeneration.

The elastic fiber degeneration score was higher in model compared with normal control mice, and the percentage of PCNA-positive cells was significantly decreased while the MMP1-positivity rate was significantly increased. All these results indicated that we successfully developed a skin photoaging nude mouse model.

CGF is a relatively recent discovery and it has thus been the subject of limited research. However, CGF has been reported to increase the proliferation and promote the osteogenic differentiation and angiogenic potential of periosteum-derived cells,<sup>25</sup> promote the proliferation, migration, and differentiation of human dental stem pulp cells exposed to lipopolysaccharide,<sup>26</sup> and increase the proliferation and secretion of neurotrophic factors by Schwann cells *in vivo*.<sup>27</sup> Our results indicated that CGF can effectively improve skin appearance and structure, alleviate pathological changes, and promote the proliferation of skin cells, leading to a therapeutic effect on skin aging.

Filoca 135HA (NCTF BOOST 135HA) was developed by Tordjman in 1978. “NCTF” refers to “New Cellular Treatment Factor”,<sup>39</sup> “BOOST” refers to “push and promote”, “135” refers to the 1988 clinical trials showing that NCTF increases the regeneration rate of human skin fiber cells by 135%, and “HA” refers to hyaluronic acid.<sup>40</sup> NCTF is a formulation containing hyaluronic acid and 53 substances,<sup>40</sup> all involved in skin aging. *In vitro* studies showed that NCTF treatment significantly improved the performance of fibroblasts and enhanced the ability of cells to resist oxidative stress.<sup>40</sup> Filoca products can currently be obtained in more than 80 countries and received Chinese Food and Drug Administration approval in 2016. We therefore, used Filoca 135HA as a positive control in the current study.

PSR technology is a new method that uses the thermal effect of plasma energy

on the skin surface to promote skin repair.<sup>41</sup> This method was first established in 2003 and has been approved by the US Food and Drug Administration for the treatment of skin wrinkles, actinic keratosis, superficial skin lesions, seborrheic keratosis, acne scars, and viral papilloma.<sup>42</sup> PSR was therefore used as another positive control in this study.

Several clinical approaches including intense pulse light, tissue filling, chemical peeling, botulinum toxin injections, and laser resurfacing have been applied to treat photoaging. Of these, intense pulsed light and laser resurfacing have shown the best results with respect to improvements in the vascular and pigmented skin lesions caused by photoaging.<sup>43</sup> Botulinum toxin injection is largely used to improve facial dynamic wrinkles and enlarged pores,<sup>43</sup> while tissue filling is mainly used to treat static wrinkles and depressed scars.<sup>43</sup> The present results showed that CGF stimulated tissue repair and regeneration through growth factors, leading to increased dermal thickness and improved wrinkles and skin elasticity. Different approaches improve different aspects of photoaging because of their distinct mechanisms of action, and a combination of these approaches can be applied, depending on the treatment objectives.

This study had some limitations. Notably, CGF was only injected once at a single concentration, and several CGF injections might result in better improvements in aging skin. Further studies are therefore needed to investigate this in the future.

In conclusion, we successfully developed a mouse model of skin photoaging using UV irradiation combined with a photosensitizer. Using this model, we tested the therapeutic effect of CGF on photoaging, and demonstrated comparable results to those of Filoca 135HA and PSR. These results suggest that CGF may have potentially

useful applications in the treatment of skin aging.

### Data availability

The datasets generated and analyzed during the current study are available from the corresponding author on reasonable request.

### Declaration of conflicting interest

The authors declare that there is no conflict of interest.

### Funding

The authors disclosed receipt of the following financial support for the research, authorship, and/or publication of this article: This work was supported by the Zhejiang Medical and Health Science and Technology Project [grant number 2016KYB086] and the Zhejiang International Science and Technology Cooperation Project [No. 2016C04003]. The authors declare that the funding body was not involved in study design, data collection, analysis, interpretation, writing of the study, or decision to submit the paper for publication.

### ORCID iD

Shusen Zheng  <https://orcid.org/0000-0003-1459-8261>

### References

1. Newton VL, McConnell JC, Hibbert SA, et al. Skin aging: molecular pathology, dermal remodelling and the imaging revolution. *G Ital Dermatol Venereol* 2015; 150: 665–674.
2. Puizina-Ivic N. Skin aging. *Acta Dermatovenerol Alp Pannonica Adriat* 2008; 17: 47–54.
3. Zhang S and Duan E. Fighting against skin aging: The way from bench to bedside. *Cell Transplant* 2018; 27: 729–738.
4. Vierkotter A and Krutmann J. Environmental influences on skin aging and ethnic-specific manifestations. *Dermatoendocrinol* 2012; 4: 227–231.

5. Parrado C, Mercado-Saenz S, Perez-Davo A, et al. Environmental stressors on skin aging. Mechanistic insights. *Front Pharmacol* 2019; 10: 759.
6. Poon F, Kang S and Chien AL. Mechanisms and treatments of photoaging. *Photodermatol Photoimmunol Photomed* 2015; 31: 65–74.
7. Trautinger F. Mechanisms of photodamage of the skin and its functional consequences for skin ageing. *Clin Exp Dermatol* 2001; 26: 573–577.
8. Sanches Silveira JE and Myaki Pedroso DM. UV light and skin aging. *Rev Environ Health* 2014; 29: 243–254.
9. Antoniou C, Kosmadaki MG, Stratigos AJ, et al. Photoaging: prevention and topical treatments. *Am J Clin Dermatol* 2010; 11: 95–102.
10. Weiss RA, Weiss MA and Beasley KL. Rejuvenation of photoaged skin: 5 years results with intense pulsed light of the face, neck, and chest. *Dermatol Surg* 2002; 28: 1115–1119.
11. Kligman DE and Zhen Y. Intense pulsed light treatment of photoaged facial skin. *Dermatol Surg* 2004; 30: 1085–1090.
12. Ping C, Xueliang D, Yongxuan L, et al. A retrospective study on the clinical efficacy of the intense pulsed light source for photodamage and skin rejuvenation. *J Cosmet Laser Ther* 2016; 18: 217–224.
13. Nelson BR, Majmudar G, Griffiths CE, et al. Clinical improvement following dermabrasion of photoaged skin correlates with synthesis of collagen I. *Arch Dermatol* 1994; 130: 1136–1142.
14. Benedetto AV, Griffin TD, Benedetto EA, et al. Dermabrasion: therapy and prophylaxis of the photoaged face. *J Am Acad Dermatol* 1992; 27: 439–447.
15. Rendon MI, Berson DS, Cohen JL, et al. Evidence and considerations in the application of chemical peels in skin disorders and aesthetic resurfacing. *J Clin Aesthet Dermatol* 2010; 3: 32–43.
16. Soleymani T, Lanoue J and Rahman Z. A practical approach to chemical peels: A review of fundamentals and step-by-step algorithmic protocol for treatment. *J Clin Aesthet Dermatol* 2018; 11: 21–28.
17. Yamauchi PS. Selection and preference for botulinum toxins in the management of photoaging and facial lines: patient and physician considerations. *Patient Prefer Adherence* 2010; 4: 345–354.
18. Borges J, Manela-Azulay M and Cuzzi T. Photoaging and the clinical utility of fractional laser. *Clin Cosmet Investig Dermatol* 2016; 9: 107–114.
19. Alves R and Grimalt R. A review of platelet-rich plasma: History, biology, mechanism of action, and classification. *Skin Appendage Disord* 2018; 4: 18–24.
20. Kobayashi E, Fluckiger L, Fujioka-Kobayashi M, et al. Comparative release of growth factors from PRP, PRF, and advanced-PRF. *Clin Oral Investig* 2016; 20: 2353–2360.
21. Conde Montero E, Fernandez Santos ME and Suarez Fernandez R. Platelet-rich plasma: applications in dermatology. *Actas Dermosifiliogr* 2015; 106: 104–111.
22. Hesselner MJ and Shyam N. Platelet-rich plasma and its utility in medical dermatology: A systematic review. *J Am Acad Dermatol* 2019; 81: 834–846.
23. Cabrera-Ramirez JO, Puebla-Mora AG, Gonzalez-Ojeda A, et al. Platelet-rich plasma for the treatment of photodamage of the skin of the hands. *Actas Dermosifiliogr* 2017; 108: 746–751.
24. Qiao J, An N and Ouyang X. Quantification of growth factors in different platelet concentrates. *Platelets* 2017; 28: 774–778.
25. Zhang L and Ai H. Concentrated growth factor promotes proliferation, osteogenic differentiation, and angiogenic potential of rabbit periosteum-derived cells in vitro. *J Orthop Surg Res* 2019; 14: 146.
26. Xu F, Qiao L, Zhao Y, et al. The potential application of concentrated growth factor in pulp regeneration: an in vitro and in vivo study. *Stem Cell Res Ther* 2019; 10: 134.
27. Qin J, Wang L, Sun Y, et al. Concentrated growth factor increases Schwann cell proliferation and neurotrophic factor secretion and promotes functional nerve recovery in vivo. *Int J Mol Med* 2016; 37: 493–500.
28. Kim TH, Kim SH, Sandor GK, et al. Comparison of platelet-rich plasma (PRP), platelet-rich fibrin (PRF), and concentrated

- growth factor (CGF) in rabbit-skull defect healing. *Arch Oral Biol* 2014; 59: 550–558.
29. Li R, Liu Y, Xu T, et al. The additional Effect of autologous platelet concentrates to coronally advanced flap in the treatment of gingival recessions: A systematic review and meta-analysis. *Biomed Res Int* 2019; 2019: 2587245.
  30. Kappes UP and Elsner P. Clinical and photographic scoring of skin aging. *Skin Pharmacol Appl Skin Physiol* 2003; 16: 100–107.
  31. Albert M. Early destructive effect of sunlight on human skin. *JAMA* 1969; 210: 2177.
  32. Dieckman LM, Freudenthal BD and Washington MT. PCNA structure and function: insights from structures of PCNA complexes and post-translationally modified PCNA. *Subcell Biochem* 2012; 62: 281–299.
  33. Benavides F, Oberyzyn TM, VanBuskirk AM, et al. The hairless mouse in skin research. *J Dermatol Sci* 2009; 53: 10–18.
  34. Fan Y, Jeong JH, You GY, et al. An experimental model design for photoaging. *J Craniofac Surg* 2015; 26: e467–e471.
  35. Kim J, Hwang JS, Cho YK, et al. Protective effects of (-)-epigallocatechin-3-gallate on UVA- and UVB-induced skin damage. *Skin Pharmacol Appl Skin Physiol* 2001; 14: 11–19.
  36. Ropke CD, Sawada TCH, Da Silva VV, et al. Photoprotective effect of Pothomorphe umbellata root extract against ultraviolet radiation induced chronic skin damage in the hairless mouse. *Clin Exp Dermatol* 2010; 30: 272–276.
  37. Aitken GR, Henderson JR, Chang SC, et al. Direct monitoring of UV-induced free radical generation in HaCaT keratinocytes. *Clin Exp Dermatol* 2007; 32: 722–727.
  38. Sumiyoshi M, Hayashi T and Kimura Y. Effects of the nonsugar fraction of brown sugar on chronic ultraviolet B irradiation-induced photoaging in melanin-possessing hairless mice. *J Nat Med* 2009; 63: 130–136.
  39. NCTF135, 135HA[product information]. Paris, France: Filorga Laboratories. Available from: <http://www.global-esthetic.com/uploads/NTCF135,135HA.pdf>.2014.
  40. Prikhnenko S. Polycomponent mesotherapy formulations for the treatment of skin aging and improvement of skin quality. *Clin Cosmet Investig Dermatol* 2015; 2015: 151–157.
  41. Foster KW, Moy RL and Fincher EF. Advances in plasma skin regeneration. *J Cosmet Dermatol* 2008; 7: 169–179.
  42. Department of Health and Human Services FaDA. 510(k)summary for the rhytec. Inc. Portraits PSIR3.
  43. Fodor L, Carmi N, Fodor A, et al. Intense pulsed light for skin rejuvenation, hair removal, and vascular lesions: a patient satisfaction study and review of the literature. *Ann Plast Surg* 2009; 62: 345–349.